

# RSC Advances



This is an *Accepted Manuscript*, which has been through the Royal Society of Chemistry peer review process and has been accepted for publication.

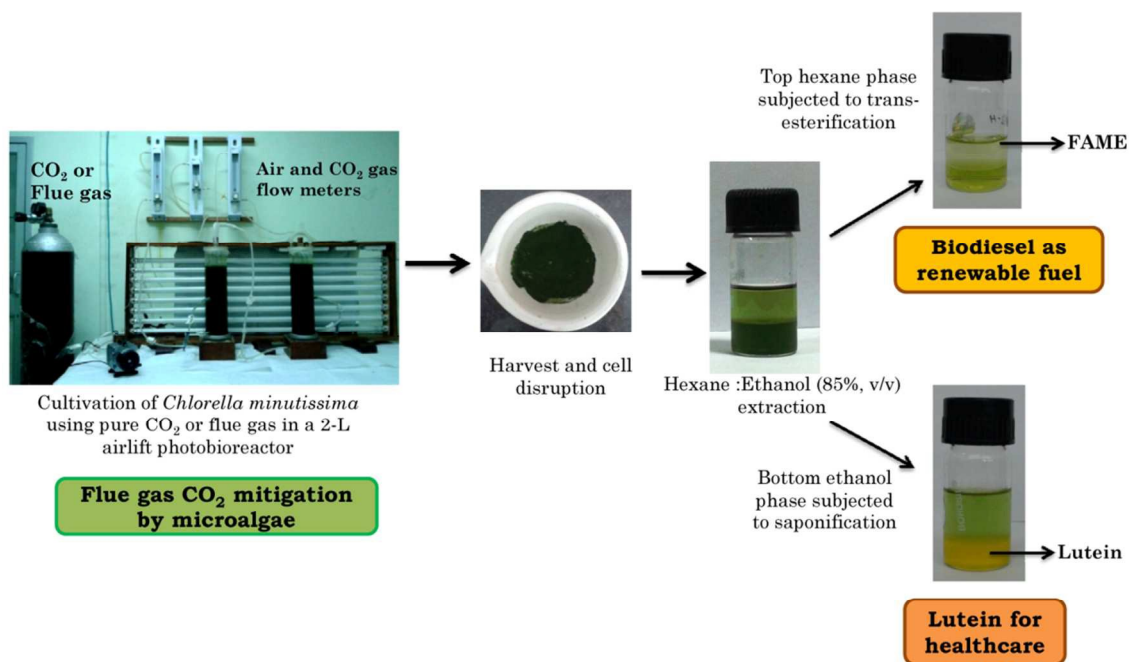
*Accepted Manuscripts* are published online shortly after acceptance, before technical editing, formatting and proof reading. Using this free service, authors can make their results available to the community, in citable form, before we publish the edited article. This *Accepted Manuscript* will be replaced by the edited, formatted and paginated article as soon as this is available.

You can find more information about *Accepted Manuscripts* in the [Information for Authors](#).

Please note that technical editing may introduce minor changes to the text and/or graphics, which may alter content. The journal's standard [Terms & Conditions](#) and the [Ethical guidelines](#) still apply. In no event shall the Royal Society of Chemistry be held responsible for any errors or omissions in this *Accepted Manuscript* or any consequences arising from the use of any information it contains.

**Highlights:**

An integrated green microalgal biorefinery was developed for concomitant flue gas CO<sub>2</sub> sequestration, lutein and lipid production for potential environmental, healthcare and biofuel applications respectively.

**Graphical Abstract**

1 **Process integration for microalgal lutein and biodiesel production with concomitant flue**  
2 **gas CO<sub>2</sub> sequestration: A biorefinery model for healthcare, energy and environment**

3 R. Dineshkumar <sup>a</sup>, Sukanta Kumar Dash <sup>b</sup>, Ramkrishna Sen <sup>a,\*</sup>

4 <sup>a</sup> Department of Biotechnology, Indian Institute of Technology Kharagpur, India

5 <sup>b</sup> Department of Mechanical Engineering, Indian Institute of Technology Kharagpur, India

6 \* Corresponding author: E-mail address: [rksen@yahoo.com](mailto:rksen@yahoo.com); Tel: +91-3222-283752

7

8 **Abstract**

9 In this study, a green microalgal feedstock based biorefinery was developed by process  
10 optimization and integration with a view to sequestering flue gas CO<sub>2</sub>, synthesizing lutein and  
11 lipid for environmental, healthcare and biofuel applications, respectively. Out of the four  
12 microalgal cultures tested in 2-L airlift photobioreactor, *Chlorella minutissima* showed  
13 comparatively higher productivities of both lutein ( $2.37 \pm 0.08 \text{ mg L}^{-1} \text{ d}^{-1}$ ) and lipid ( $84.3 \pm 4.1$   
14  $\text{mg L}^{-1} \text{ d}^{-1}$ ). Upon optimization of the critical process parameters using artificial neural network  
15 modeling and particle swarm optimization (ANN-PSO) technique, the productivities of lutein  
16 and lipid were enhanced to  $4.32 \pm 0.11 \text{ mg L}^{-1} \text{ d}^{-1}$  and  $142.2 \pm 5.6 \text{ mg L}^{-1} \text{ d}^{-1}$  respectively, using  
17 pure CO<sub>2</sub> sequestered at a rate of  $1.2 \pm 0.03 \text{ g L}^{-1} \text{ d}^{-1}$ . One of the most interesting findings was  
18 that lutein and lipid productivities were not significantly affected by the use of toxic flue-gas,  
19 when diluted to 3.5% CO<sub>2</sub> with air, under the same process conditions, suggesting possible  
20 commercial usefulness of flue-gas carbon. Another major achievement is that a single step  
21 ethanol-hexane based extraction procedure, followed by parallel saponification and trans-  
22 esterification, resulted in simultaneous recovery of 94.3% lutein and 92.4% fatty acid methyl

1 ester. Therefore, potential industrial significance of this study lies in the development of an  
2 integrated biorefinery that may prove to be a sustainable technology platform towards addressing  
3 some contemporary challenges in healthcare, energy and environment through concomitant  
4 production of microalgal lutein as a nutraceutical and biodiesel as an alternative fuel, coupled  
5 with flue gas CO<sub>2</sub> sequestration.

6 **Keywords:** Microalgal biorefinery; Lutein; Lipid; Biodiesel; Flue gas; CO<sub>2</sub> sequestration;  
7 Process integration.

## 8 **1. Introduction**

9 Microalgae have been considered as the potent photosynthetic microorganisms, as they are  
10 envisaged to solve the challenges of food, feed and fuels production in the near future.<sup>1</sup>  
11 Moreover, they serve as a sustainable and potential alternative for remediating waste water,  
12 sequestering flue gas CO<sub>2</sub>, and producing many high-value products such as carotenoids, poly  
13 unsaturated fatty acids, exo-polysaccharides, antioxidants and vitamins.<sup>1-3</sup> Lutein, one of the  
14 commercially important carotenoids, has gained increasing attention due to its various health  
15 care applications including prevention and amelioration of age related blindness, cataracts,  
16 certain types of cancers and atherosclerosis.<sup>4</sup>

17 A majority of works reported in the literatures have focused on directing the microalgal  
18 cultivation for one particular application; either producing a commercially important product or  
19 to sequester CO<sub>2</sub> from the pollutant gas. This makes the microalgal cultivation economically  
20 unattractive for commercial applications.<sup>5, 6</sup> Hence, it is important to have an integrated  
21 biorefinery approach that can serve three purposes. For instance, sequestration of CO<sub>2</sub> by  
22 microalgae, a sustainable pollution mitigation strategy, can be coupled to the simultaneous

1 production of two products; a high-volume, low-value product like lipid for biodiesel and a  
2 low-volume, high-value pigment like lutein for healthcare applications. However, this strategy  
3 is primarily dependent on the type of microalgal species. For example, microalgae of  
4 chlorophycean class are one of the potential strains that have been reported to accumulate  
5 significant proportion of both carotenoids (lutein) and lipid, in addition to their CO<sub>2</sub>  
6 sequestration potential.<sup>7,8</sup>

7 One of the key issues in the simultaneous production of lutein and lipid is the influence of  
8 nitrogen source availability or timing of cell harvest. Generally, the accumulation of lutein  
9 reaches its maximum level near the onset of nitrogen depletion in the medium,<sup>9</sup> whereas, the  
10 maximum lipid accumulation is achieved upon nitrogen starved conditions.<sup>10,11</sup> As a result, the  
11 maximum production of both lutein and lipid might not occur at the same cultivation time.  
12 Moreover, it is difficult to obtain the optimal process conditions for enhancing both lutein and  
13 lipid.<sup>12</sup> Therefore, the harvesting time and optimal conditions for improved product synthesis  
14 will be mainly dependent on which product is preferred to be produced. In the current study,  
15 lutein was considered as the primary target product as it is a growth-associated and high-value  
16 product. Accordingly, the optimal process conditions and cultivation time was prioritized for  
17 improving lutein synthesis, while lipid was also obtained as a co-product. The other critical issue  
18 in this process integration study is to extract and recover both lutein and lipid simultaneously  
19 from the biomass. It has to be noted that there are very few reports which demonstrate the  
20 feasibility of recovering two products concomitantly from the microalgal biomass.

21 Prommuak et al.<sup>13</sup> reported the simultaneous recovery of lutein and biodiesel from *Chlorella*  
22 *vulgaris*. They observed that the alkali catalyst used for transesterification of lipids also  
23 converted the lutein esters to free lutein at appropriate conditions. In another study, Bai et al.<sup>14</sup>

1 investigated the feasibility of concomitant separation of chlorophylls and lipids from *Chlorella*  
2 *pyrenoidosa*, using an appropriate solvent mixture based on solubility nature of the products.  
3 However, the novelty of our study lies in the integrated biorefinery approach that can serve three  
4 purposes at a time, namely, concomitant production of microalgal lutein and biodiesel along with  
5 CO<sub>2</sub> sequestration. Once the integrated biorefinery concept has been developed, the process can  
6 be scaled up by maintaining the universal scale up parameters like P/V (power consumed per  
7 unit reactor volume) and K<sub>L</sub>a (volumetric mass transfer coefficient). For instance, the optimal  
8 flow rate or superficial gas velocity that will be determined from this study can be used to  
9 calculate P/V, which is one of the critical scale-up criteria. However, the development of low-  
10 cost large scale photobioreactors, cost-effective cell separation and downstream processing  
11 techniques are essential, in order to improve the competitiveness of commercially important  
12 microalgal products and the overall process economically feasible.<sup>5</sup> The use of low-cost sources  
13 of CO<sub>2</sub>, nutrients and water would likely to reduce the cost involved in microalgal biomass  
14 cultivation by more than 50% and also mitigate the pollutants considerably.<sup>5</sup> Hence, in the  
15 current study, flue gas was used as the viable alternative source of CO<sub>2</sub> for microalgal  
16 cultivation.

17 Thus, the present study was aimed at designing and integrating the bioprocesses for  
18 microalgae mediated flue gas CO<sub>2</sub> sequestration with concomitant production of lutein and  
19 biodiesel in a biorefinery model. This requires the implementation of the following strategies,  
20 namely, (i) selecting a suitable microalgal species which can yield higher productivities of both  
21 lutein and lipid, (ii) optimizing the most influential process parameters for improving the  
22 productivities of lutein as primary target product and lipid, using an advanced mathematical  
23 modeling and optimization technique, and (iii) integrating the processes of flue gas CO<sub>2</sub>

1 sequestration with the concurrent recovery of lutein and biodiesel under the optimized process  
2 conditions.

## 3 **2. Materials and Methods**

### 4 **2.1. Microalgae and culture conditions**

5 Four green microalgal strains of chlorophycean class were used in this work and are as  
6 follows: *Chlorella minutissima* (MCC-27) from Indian Agricultural Research Institute, New  
7 Delhi; *Scenedesmus* sp. *Chlorella* sp. and *Chlorococcum* sp. were kindly provided by Institute of  
8 Bio-resources and Sustainable Development, Imphal, India. These strains show high growth rate  
9 at pH 7–9 and temperature 25–32 °C. The modified Bold's Basal medium (BBM) which was  
10 standardized earlier<sup>15</sup> for yielding higher lutein productivity, was used in this screening and  
11 optimization study.

### 12 **2.2. Design and operation of photobioreactor**

13 A 2-L airlift photobioreactor was appropriately designed for culturing microalgae and the  
14 design parameters are as follows: height/diameter, 3.6; illuminated surface area/volume, 0.465  
15 cm<sup>-1</sup>; area of downcomer/area of riser, 1.25 and perforated ring shaped spargers with  $\Phi_{\text{sparger}}$ , 5.5  
16 cm and  $\Phi_{\text{pore}} = 0.5$  mm. The photobioreactor was equipped with cool white fluorescent lamps  
17 that were mounted on both sides of the reactor. All the screening and optimization experiments  
18 were performed in this photobioreactor in batch mode using the modified BBM with the  
19 following cultivation conditions: inoculum concentration, 50 mg L<sup>-1</sup>; inoculum age, mid-log  
20 phase; pH, 7–8 and temperature, 30 ± 2 °C. The microalgal biomass was harvested near the onset  
21 of nitrogen depletion in the culture medium for all experiments.

### 22 **2.3. Optimization of process conditions**

1 The selected lutein and lipid rich microalga was considered for further improvement of lutein  
2 and lipid productivities. In some cases, the complex non-linear biological interactions cannot be  
3 completely explained by using second-order polynomial model involving response surface  
4 methodology.<sup>16, 17</sup> Hence, we implemented artificial neural network modeling (ANN) coupled  
5 with particle swarm optimization (PSO) technique for determining the optimum levels of critical  
6 process parameters for improved productivities of lutein (main response) and lipid.

7 The process parameters that critically influence the productivities of lutein and lipid were  
8 identified as light intensity, CO<sub>2</sub> concentration and air flow rate. These parameters also influence  
9 the performance of photobioreactor in terms of irradiance, mass transfer, mixing and  
10 hydrodynamic characteristics.<sup>18</sup> Indeed, the availability of nitrogen in medium affects the  
11 accumulation of lutein and lipid inversely in microalgae. However, the rate of lipid accumulation  
12 (lipid productivity) is reduced considerably for the microalgae grown under nitrogen exhausted  
13 medium.<sup>2, 7</sup> Moreover, the optimal nitrate concentration (13.55 mM) that was determined from  
14 our previous study<sup>15</sup> for enhanced lutein productivity, is corroborated with the study of  
15 Abdelaziz et al.<sup>19</sup> They reported that the nitrate concentration of 11.5 mM was required for  
16 maximizing lipid productivity in a green microalga *Chlorella*. Hence, nitrate concentration was  
17 not included in the experimental design, considering lutein as primary target product.

18 The experimental range and levels of the selected parameters are shown in Supplementary  
19 Table A.1. A central composite design (CCD) matrix was constructed for three factors (light  
20 intensity, CO<sub>2</sub> concentration and air flow rate) and the experimental design (Table 2) was  
21 obtained using Design Expert version 7.1.3 (Stat-Ease Inc., Minneapolis, USA). The  
22 experimental design that consists of 20 runs was carried out using 2-L airlift photobioreactor



1 (batch mode) in duplicates. The experimental data obtained from CCD were used for developing  
2 the neural network model and subsequently optimized by PSO technique.

3 ANN is applied in almost all engineering fields for the modeling of multivariate non-linear  
4 processes. Because of its robustness and ability to simulate complex biological processes more  
5 accurately, ANN has found application in process biotechnology.<sup>17</sup> This model can be evaluated  
6 using mean squared error (MSE) as performance index (Eq. (1)) and overall correlation  
7 coefficient (R) as precision of the model.

$$8 \quad MSE = \sum \frac{(Experimental\ value - predicted\ value)^2}{n} \quad (1)$$

9 PSO, a contemporary evolutionary algorithm, is basically inspired by the migration patterns  
10 of living creatures like bird flocking and fish schooling. It has recently been applied to optimize  
11 complex multivariate non-linear bioprocess, because of its properties such as faster inter-particle  
12 communication, rapid data processing and easy implementation. Owing to its ability to sort out  
13 best fitness values even after several iterations, it is believed to be superior to other  
14 computational evolutionary algorithm like genetic algorithm.<sup>16</sup> It updates its velocity and  
15 position at different time intervals according to Eqs. (2) and (3), respectively.

$$16 \quad V_i^k = w^{k-1} + V_i^{k-1} + C_1 R_1 (L_i^{k-1} - P_i^{k-1}) + C_2 R_2 (G_i^{k-1} - P_i^{k-1}) \quad (2)$$

$$17 \quad P_i^k = P_i^{k-1} + V_i^k \quad (3)$$

18 where,  $V_i^k$  and  $V_i^{k-1}$  are velocities of particle  $i$  at iteration  $k$  and  $k-1$ , respectively;  $C_1$  and  $C_2$ ,  
19 learning factors;  $w^{k-1}$ , inertia weight;  $R_1$  and  $R_2$ , uniformly distributed random variables between  
20 0 and 1;  $L_i^{k-1}$ , local best solution of particle  $i$ ;  $G_i^{k-1}$ , global best solution of the group;  $P_i^k$  and  $P_i^{k-1}$

1 are positions of particle  $i$  at iteration  $k$  and  $k-1$ , respectively. The working principles of ANN-  
2 PSO for optimization of bioprocesses are discussed in earlier reports.<sup>15, 16</sup> The computation of  
3 ANN-PSO was performed by using MATLAB version 8.0 (Mathworks Inc., Natick, USA).

## 4 **2.4. Process integration**

### 5 **2.4.1. Flue gas generator and storage setup**

6 An indigenously designed *in situ* flue gas generator and suction devices was used in this  
7 study. The coal required for flue gas sequestration study was kindly provided by Kolaghat  
8 Thermal Power Station (KTPS), West Bengal, India. The KTPS coal was burnt in the furnace,  
9 and water circulation via double jacketed layer was provided to cool-down the emitted gas. The  
10 flue gas, which was emitted at the chimney, was captured and passed to a filter mesh to remove  
11 the suspended particles, and then stored in cylinders through appropriate suction and compressor  
12 pumps. The composition of flue gas was measured using online flue gas analyzer (Model: FGA  
13 53X; Make: INDUS Scientific, Mumbai, India) and they are as follows: CO<sub>2</sub>, 12%; CO, 0.55%;  
14 O<sub>2</sub>, 8.33%; NO<sub>2</sub>, 63.8 ppm; SO<sub>x</sub>, 61.9 ppm and HC, 9 ppm.

### 15 **2.4.2. Microalgae mediated flue gas CO<sub>2</sub> sequestration process**

16 Once the process conditions were optimized in lab conditions, the selected microalga was  
17 grown using diluted-flue gas, which corresponds to the optimal CO<sub>2</sub> (%) as determined by  
18 ANN-PSO technique. This experiment was carried out in batch mode at closed-outdoor  
19 conditions (near flue gas generation facility) with artificial irradiance supply (light intensity as  
20 predicted by ANN-PSO) at the temperature range between 27 °C and 33 °C.

### 21 **2.4.3. Optimization of binary solvent system for simultaneous recovery of lutein and** 22 **biodiesel**

1 The solubility of lutein in different solvents was systematically studied by Craft and Soares.<sup>20</sup>  
2 They found that the xanthophyll lutein was sparingly soluble in hexane due to the presence of  
3 dihydroxy groups, while it exhibited comparatively higher lutein solubility in polar solvents like  
4 ethanol, methanol and 2-propanol. It is also known that the non-polar solvent like hexane can  
5 effectively separate neutral lipid fraction from the crude lipid.<sup>21, 22</sup> In our study, an appropriate  
6 binary solvent system involving organic and aqueous phases having different solubilities towards  
7 neutral lipids and lutein was used for the separation. To identify the suitable solvent system that  
8 can effectively separate these two products from the biomass, three binary solvent systems (each  
9 at a ratio of 1:1) namely methanol–hexane, ethanol–hexane and 2-propanol– hexane, were tested.  
10 A suitable quantity of water was added to each of these binary solvent systems to obtain two  
11 layers; lipid rich upper organic hexane phase and lutein rich bottom aqueous alcoholic phase. For  
12 effective separation of lipids and lutein, the organic and aqueous phases were extracted twice  
13 with their respective aqueous and organic phases. Finally, the pooled phases were subjected to  
14 the following reactions; the organic phase containing lipid to trans-esterification and the aqueous  
15 alcoholic phase to saponification to obtain pure lutein. The products from these two reactions  
16 were then quantified using the protocols as discussed in Section 2.5. In order to calculate the  
17 recovery efficiency of the products that obtained through this simultaneous recovery method, a  
18 known amount of biomass was also taken separately to estimate the lutein and FAME contents,  
19 as per the protocols mentioned below and were labeled as control.

## 20 **2.5. Analytical procedures**

21 The biomass concentration was estimated at OD<sub>750 nm</sub> and gravimetrically. The concentration  
22 of nitrate was determined according to Ho et al.<sup>23</sup> The carotenoids extraction and saponification  
23 reaction to obtain pure lutein were carried out as described in Dineshkumar et al.<sup>15</sup> Subsequently,

1 lutein was quantified using reverse phase High Performance Liquid Chromatography (Agilent,  
 2 USA). The total lipid content of the microalgae was measured according to Bligh and Dyer.<sup>24</sup>  
 3 The lipid was then trans-esterified using 3-N methanolic HCl at 70° C for 5 h and extracted into  
 4 hexane phase. The transesterification of lipids and quantification of fatty acid methyl ester  
 5 (FAME), were performed by following the procedure of Sheng et al.<sup>25</sup>

6 The gas chromatography (Thermo Fisher Scientific–Chemito Ceres 800 plus) with BPX 70  
 7 capillary column (30 m × 0.25 mm), was used for identification and quantification of FAME.  
 8 The operating conditions are as follows: injector temperature, 260 °C; detector temperature, 280  
 9 °C; injection volume, 1 µl; split ratio: 1:25 and oven temperature started at 70 °C for 1 min,  
 10 increased at 5 °C/min to 180 °C for 10 min and 6 °C /min to 220 °C for 11 min. The standards  
 11 such as lutein (Sigma–Aldrich) and FAME–Mix 37 component (Supelco) were used for  
 12 quantification of respective products.

$$\text{FAME content} = \frac{\text{Amount of FAME obtained (mg)}}{\text{Amount of biomass taken (g)}} * 100$$

$$\text{FAME yield} = \frac{\text{Amount of FAME obtained (mg)}}{\text{Amount of CO}_2 \text{ consumed (g)}} * 100$$

13 The elemental composition of microalgal biomass (CHNS) was determined using a Vario  
 14 MACRO Cube elemental analyzer (Elementar Analysensysteme GmbH, Germany Make). The  
 15 general empirical chemical formula of the microalgal biomass is  $\text{CH}_{1.83}\text{N}_{0.11}\text{O}_{0.48}\text{P}_{0.01}$ <sup>26</sup>. The  $\text{CO}_2$   
 16 fixation rate in microalgal biomass was calculated by using Eq. (4)  
 17  $\text{CO}_2$  fixation rate ( $\text{gL}^{-1}\text{d}^{-1}$ ) = Carbon content(%) \* Biomass productivity ( $\text{gL}^{-1}\text{d}^{-1}$ ) \*  $\frac{44}{12}$  (4)

18 The photosynthetic efficiency (P.E) was determined using (Eq. (5))

$$1 \quad P.E(\%) = \frac{\text{Biomass growth (gd}^{-1}\text{)} * \text{Enthalpy of biomass (KJ g}^{-1}\text{)}}{\text{Irradiance (\mu mol m}^{-2}\text{ s}^{-1}\text{)} * \text{Illuminated surface area (m}^2\text{)} * \text{Conversion factor (18.78 KJs d}^{-1}\text{)}} * 100 \quad (5)$$

2 The total chlorophyll and carotenoids were extracted using methanol and estimated according to  
3 Welburn<sup>27</sup> (Eqns. (6) to (9)).

$$4 \quad \text{Chlorophylla}(C_a) = 15.65A_{666} - 7.34A_{653} \quad (6)$$

$$5 \quad \text{Chlorophyllb}(C_b) = 27.05A_{653} - 11.21A_{666} \quad (7)$$

$$6 \quad \text{TotalChlorophyll}(mgL^{-1}) = C_a + C_b \quad (8)$$

$$7 \quad \text{TotalCarotenoids}(mgL^{-1}) = \frac{1000A_{470} - 2.86C_a - 129.2C_b}{221} \quad (9)$$

### 8 **3. Results and Discussion**

#### 9 **3.1. Comparison of lutein, lipid and biomass productivities of four chlorophycean** 10 **microalgal strains**

11 As the green microalgal species are rich in carotenoids and lipids and also exhibit high  
12 growth rate, they are generally recognized as one of the potential candidates for lutein and  
13 biodiesel production.<sup>1,8</sup> In the present study, four green microalgal strains that were identified as  
14 better performing strains in our laboratory, were compared for their accumulation of both lipid  
15 and lutein. The parameters such as biomass growth and lutein and lipid production of these  
16 microalgal strains were examined at the following operating conditions: light intensity, 100  $\mu\text{mol}$   
17  $\text{m}^{-2}\text{ s}^{-1}$ ;  $\text{CO}_2$  concentration, 2 %; flow rate, 0.35 vvm ( $700\text{ ml min}^{-1}$ ); temperature, 30 °C and pH,  
18 7–8. For a better comparison, the efficiency of the production process was assessed in terms of  
19 productivity ( $\text{mg L}^{-1}\text{ d}^{-1}$ ), as reported by Xie et al.<sup>9</sup>

1 As discussed earlier, the four microalgal strains were harvested when the nitrogen source was  
2 about to be depleted in the medium. It was observed that the specific growth rate and the lutein  
3 productivity were higher for *Chlorella minutissima* and *Scenedesmus* sp, followed by *Chlorella*  
4 sp and *Chlorococcum* sp (Table 1). The microalga *C. minutissima* showed the highest lipid  
5 productivity (84.3 mg L<sup>-1</sup> d<sup>-1</sup>), followed by *Chlorococcum* sp (81.9 mg L<sup>-1</sup> d<sup>-1</sup>), *Scenedesmus* sp  
6 (71.8 mg L<sup>-1</sup> d<sup>-1</sup>) and *Chlorella* sp (56.5 mg L<sup>-1</sup> d<sup>-1</sup>). Among the tested microalgal species, *C.*  
7 *minutissima* was observed to yield higher productivities of both lutein (2.37 mg L<sup>-1</sup> d<sup>-1</sup>) and lipid  
8 (84.3 mg L<sup>-1</sup> d<sup>-1</sup>), with the specific growth rate of 1.44 d<sup>-1</sup> and CO<sub>2</sub> fixation rate of 0.73 g L<sup>-1</sup> d<sup>-1</sup>  
9 (Table 1). Therefore, the strain *C. minutissima* was chosen for subsequent biorefinery study  
10 involving process optimization and integration.

### 11 **3.2. Optimization of critical process parameters for improved lutein and lipid** 12 **productivities**

13 Although the cultivation of *C. minutissima* resulted in higher lutein and lipid productivities  
14 among the tested strains, these productivities was found to be relatively lower, as compared to  
15 that of reported in the relevant literature. In general, the increase in light intensity and CO<sub>2</sub> result  
16 in enhanced productivities of both lutein and lipid from microalgae.<sup>4, 28</sup> Hence, it is essential to  
17 optimize the key parameters such as light intensity, CO<sub>2</sub> concentration and flow rate that  
18 significantly influence the microalgal growth rate, CO<sub>2</sub> sequestration rate and photobioreactor  
19 performance. As discussed in Section 2.3, the optimal nitrate concentration that was previously  
20 determined for yielding higher lutein productivity was added to the medium, considering lutein  
21 as primary target product. Consequently, nitrate concentration was not included in the  
22 experimental design. Table 2 shows the productivities of lutein, lipid and biomass for different  
23 combinations of the critical process parameters.

### 1        **3.2.1. Optimization of process parameters by ANN–PSO technique**

2        The ANN model with lutein productivity as the primary objective was constructed by  
3        assigning the obtained CCD data (Table 2) as follows: training, 70%; testing, 15% and  
4        validation, 15%. The additional data points needed for training the neural network were  
5        generated using the regression equation (Supplementary Eq. A.1), as suggested by Maji et al.<sup>29</sup>  
6        The ANN–topology consists of three layers: input layer with 3 neurons representing the input  
7        parameters; output layer with one neuron that corresponds to the main objective (lutein  
8        productivity), and a layer between input and output layers called hidden layer, wherein the  
9        number of neurons needs to be determined for developing an efficient topology. The  
10       performance of ANN is primarily dependent on the type of training algorithm and the transfer  
11       functions employed at the hidden and output layers, while training the network. The accuracy of  
12       the ANN model was evaluated in terms of mean squared error (MSE) and overall correlation  
13       coefficient (R).

14       In this investigation, we found that the best performance was obtained using feed–forward  
15       back propagation training algorithm with the log–sigmoidal and linear transfer functions at the  
16       hidden and output layers respectively, in terms of low–MSE value (0.0004) and the maximum  
17       R–value of 0.995 (Fig. 1a). The use of optimal neuron number in the hidden layer is critical in  
18       achieving the best neural network architecture. Consequently, the required number of neurons  
19       was optimized as reported by Huang et al<sup>17</sup>. In our study, we found that the critical number of  
20       neurons in the hidden layer was 7 with respect to MSE and R- values (Supplementary Fig. A.1).  
21       Hence, 3–7–1 ANN topology (Fig. 1b) was selected. This model was validated by performing  
22       additional experiments that were different from Table 2. It was observed that the prediction error  
23       between the simulated and experimental outputs was within 3.2% (Supplementary Table A.2).

1 This indicated the accuracy of 3–7–1 ANN topology and thus, this developed model was used as  
2 a fitness function in PSO algorithm for predicting the optimal combinations of process  
3 parameters for enhanced lutein productivity.

4 The critical parameters of PSO algorithm such as population size, inertia weight and learning  
5 factors, were estimated as described in earlier reports.<sup>16</sup> It was observed that all the particles  
6 converged to the global optimal solution of 4.45 mg L<sup>-1</sup> d<sup>-1</sup> in less than 50 iterations (Fig. 1c) for  
7 the following combinations of input process parameters: light intensity, 260 μmol m<sup>-2</sup> s<sup>-1</sup>; CO<sub>2</sub>  
8 concentration, 3.5% and flow rate, 850 mL min<sup>-1</sup> (0.425 vvm). Further, the efficiency of PSO  
9 technique was validated by performing the validation experiment with the above mentioned  
10 values of input parameters. The experimentally tested lutein productivity resulted in 4.32 ± 0.11  
11 mg L<sup>-1</sup> d<sup>-1</sup>, which was in close agreement with the simulated output (~3% error).

12 Thus, the application of ANN–PSO approach for optimization of key process parameters  
13 significantly enhanced the lutein productivity from 2.37 to 4.32 mg L<sup>-1</sup> d<sup>-1</sup> (82% improvement).  
14 Moreover, the biomass productivity was increased from 0.407 to 0.67 g L<sup>-1</sup> d<sup>-1</sup> (60%  
15 enhancement) and the total lipid productivity was improved from 84.3 to 142.2 mg L<sup>-1</sup> d<sup>-1</sup> (69%  
16 increment). This indicated that the selected process parameters drastically influenced both lutein  
17 and lipid synthesis in *C. minutissima*. The effect of critical process parameters on lutein and lipid  
18 production is discussed in Section 3.2.2. Although the resulted lutein productivity (4.32 mg L<sup>-1</sup>  
19 d<sup>-1</sup>) is comparable with that of literature, the lutein content (6.37 mg g<sup>-1</sup>) obtained in this study is  
20 significantly higher than that of reported in the relevant batch studies. Further, the resulted lipid  
21 productivity (142.2 mg L<sup>-1</sup> d<sup>-1</sup>) and content (21.2%) can be reasonably compared with the studies  
22 reported for lipid productivity obtained upon nitrogen starvation conditions.<sup>7, 10, 28</sup> For instance,  
23 the maximum lipid productivity of 140.35 mg L<sup>-1</sup> d<sup>-1</sup> (content, 22.4%) was obtained by



1 *Scenedesmus obliquus* under 5-day nitrogen starvation period.<sup>28</sup> Thus, these results demonstrate  
2 the usefulness of this optimization strategy for improving the productivities of lutein and lipid. In  
3 addition, it has to be noted that this microalga *C. minutissima* can be considered as a potential  
4 candidate for the production of both lutein and lipid in a biorefinery model.

### 5 **3.2.2. Effect of critical process parameters on lutein, lipid and biomass productivities**

6 The process parameters such as light intensity, CO<sub>2</sub> supply and aeration rate significantly  
7 influenced the synthesis of lutein and lipid in *C. minutissima*. Light acts as an important energy  
8 source for the photo-autotrophic microalgae and its intensity level strongly influences the growth  
9 rate and product accumulation.<sup>1, 8</sup> This is evident from our study that the increase in light  
10 intensity from 50 to 250  $\mu\text{mol m}^{-2} \text{s}^{-1}$  resulted in significant enhancement in the productivities of  
11 lutein (from 1.05 to 4.13  $\text{mg L}^{-1} \text{d}^{-1}$ ), biomass (from 0.218 to 0.596  $\text{g L}^{-1} \text{d}^{-1}$ ) and lipid (from 21.1  
12 to 126.5  $\text{mg L}^{-1} \text{d}^{-1}$ ) (Fig. 2a). The increased lutein synthesis might be attributed to the light  
13 induced rapid up-regulation of carotenoid biosynthesis genes such as phytoene synthase and  
14 phytoene desaturase.<sup>30</sup> Moreover, the improvements in lipid productivity and CO<sub>2</sub> fixation rate  
15 were mostly associated with the increase of biomass productivity, as reported by Ho et al.<sup>28</sup>

16 The increase in light intensity from 250 to 300  $\mu\text{mol m}^{-2} \text{s}^{-1}$  improved the productivities of  
17 biomass and lipid moderately; however, the lutein productivity dropped slightly. The decrease in  
18 lutein accumulation at higher light intensity may be due to the size reduction of light-harvesting  
19 receptors, where the lutein is predominantly present.<sup>23</sup> Moreover, the photosynthetic efficiency,  
20 which is the ratio of light energy recovered by biomass to the amount of light energy supplied,  
21 was observed to decrease steadily from 10.97 to 5.7%, with the increase in light intensity from

1 50 to 300  $\mu\text{mol m}^{-2} \text{s}^{-1}$  (Fig. 2a). Thus, the optimal light intensity of 260  $\mu\text{mol m}^{-2} \text{s}^{-1}$  for  
2 enhanced product synthesis in *C. minutissima* was suitably predicted by PSO technique.

3  $\text{CO}_2$  serves as an exclusive carbon source for autotrophic microalgae. The concentration of  
4  $\text{CO}_2$  (% v/v) and the aeration rate ( $\text{mL min}^{-1}$ ) drastically affect the mass transfer rate and  $\text{CO}_2$   
5 fixation rate in microalgal biomass.<sup>31</sup> The amount of  $\text{CO}_2$  present in the air (0.04%) is inadequate  
6 to achieve the high-density cultures and on the other hand, excess supply of  $\text{CO}_2$  may inhibit the  
7 carbonic anhydrase enzyme<sup>32</sup>, thereby reducing the biomass productivity. As shown in Fig. 2b,  
8 increasing the concentration of  $\text{CO}_2$  in the inlet gas from 0.8 to 2.5% improved the efficiency of  
9 microalgal photosynthesis (from 4.19 to 8.05%),  $\text{CO}_2$  fixation rate (from 0.519 to 1.01  $\text{g L}^{-1} \text{d}^{-1}$ )  
10 and the productivities of lutein (from 2.18 to 3.41  $\text{mg L}^{-1} \text{d}^{-1}$ ) and lipid (from 69.7 to 95.1  $\text{mg L}^{-1}$   
11  $\text{d}^{-1}$ ). However, the further increase in  $\text{CO}_2$  (>5%) negatively influenced the photosynthesis. This  
12 is evident from the fact that increase in  $\text{CO}_2$  concentration up to a critical level would enhance  
13 the activity of enzymes such as carbonic anhydrase and Rubisco<sup>33</sup> and hence, improves the  
14 photosynthesis. A high  $\text{CO}_2$  supply inhibits the critical enzymes involved in photosynthesis  
15 process, as a result of significant drop in pH of the medium below the critical level<sup>32</sup>, affecting  
16 the cell growth rate. Therefore, in this study, the optimal  $\text{CO}_2$  of 3.5% (v/v) for enhanced growth  
17 rate and product accumulation in *C. minutissima* was satisfactorily determined by PSO  
18 technique. This value is in close agreement with the optimal  $\text{CO}_2$  (4%) reported by Nakanishi et  
19 al.<sup>7</sup> for the enhanced lipid productivity (169.1  $\text{mg L}^{-1} \text{d}^{-1}$ ) by *Chlamydomonas* sp. JSC4.

20 The third influencing factor is aeration rate and it plays crucial roles such as minimizing  
21 photo-limitation or shelf-shading in high-density cultures, distributing the nutrients  
22 homogeneously in the culture medium, and maximizing  $\text{CO}_2$  dissolution and  $\text{O}_2$  evolution.<sup>33</sup> In  
23 the current study, the cultivation of *C. minutissima* in customized airlift photobioreactor for

1 aeration rates in the range of 395 to 600 mL min<sup>-1</sup> resulted in poor mixing and gas-liquid mass  
2 transfer. Thus, low yields of biomass, lipid and lutein were obtained (Fig. 2c). When the aeration  
3 rate was increased to 900 mL min<sup>-1</sup>, remarkable improvements were observed for photosynthetic  
4 efficiency (from 4.17 to 7.78%), CO<sub>2</sub> fixation rate (from 0.52 to 0.96 g L<sup>-1</sup> d<sup>-1</sup>), lutein  
5 productivity (from 2.27 to 3.57 mg L<sup>-1</sup> d<sup>-1</sup>) and lipid productivity (39.6 to 97.8 mg L<sup>-1</sup> d<sup>-1</sup>) (Fig.  
6 2c). However, when the flow rate was further increased ( $\geq$  1200 mL min<sup>-1</sup>), the productivities of  
7 biomass, lipid and lutein were found to be reduced, which may be due to shear stress to the cells.  
8 The another probable reason is that the higher flow rates tend to reduce the retention time of gas  
9 bubbles and thereby decreasing the utilization of CO<sub>2</sub> by the microalgal cells.<sup>31</sup> Hence, the  
10 optimum aeration rate of 850 mL min<sup>-1</sup> (0.425 vvm) for improved product synthesis in *C.*  
11 *minutissima* was adequately determined by PSO technique.

### 12 **3.3. Process integration for the development of microalgal biorefinery model**

#### 13 **3.3.1. Microalgae mediated flue gas CO<sub>2</sub> mitigation**

14 In this study, the microalga *C. minutissima* was grown using flue gas under the optimized  
15 conditions, as determined by ANN-PSO technique. The concentration of CO<sub>2</sub> present in the flue  
16 gas (12% CO<sub>2</sub>) was appropriately diluted to 3.5% (optimal CO<sub>2</sub> %, v/v) with inlet air using  
17 suitable gas flow meters. Although *C. minutissima* could be grown effectively using undiluted  
18 flue gas, it was presumed that the loss of CO<sub>2</sub> from the photobioreactor could be significantly  
19 reduced by sparging diluted-flue gas. This experiment was performed near the flue gas  
20 generation facility (closed-outdoor conditions) and artificial illumination of 260  $\mu\text{mol m}^{-2} \text{s}^{-1}$   
21 (optimal light intensity) was continuously supplied. However, the temperature was left  
22 uncontrolled and it was found to vary between 27 °C and 33 °C.

1 The experimental setup of CO<sub>2</sub> sequestration by *C. minutissima* under the optimized process  
2 conditions is shown in Supplementary Fig.A.2. Fig. 3a and b illustrates the time-course profiles  
3 for biomass production, CO<sub>2</sub> fixation rate, productivities of lutein and lipid, and nitrate uptake  
4 under pure CO<sub>2</sub> and flue gas cultivation conditions. The microalga *C. minutissima* was observed  
5 to utilize the flue gas CO<sub>2</sub> as the carbon source effectively. Moreover, the diluted flue gas with  
6 reduced amounts of NO<sub>x</sub> and SO<sub>x</sub> did not significantly affect the growth rate of microalga. This  
7 is in accordance with the study of Kao et al.<sup>34</sup>, which reported that the dilution of flue gas with  
8 air is essential to maximizing the efficiency of CO<sub>2</sub> removal and the productivities of biomass  
9 and lipid in *Chlorella* sp. MTF-15.

10 In the present study, the maximum biomass, lutein and lipid productivities of flue gas aerated  
11 cultures were found to be 0.64 g L<sup>-1</sup> d<sup>-1</sup>, 4.15 mg L<sup>-1</sup> d<sup>-1</sup> and 139.3 mg L<sup>-1</sup> d<sup>-1</sup>, respectively (Table  
12 3). These productivities were found to be almost consistent with that of pure CO<sub>2</sub> (3.5%) sparged  
13 cultures of *C. minutissima* (Fig.3a and b). To the best of our knowledge, this is the first report  
14 that investigates the production of lutein from flue gas grown microalgae. Hence, the further  
15 characterization of the product lutein from flue gas grown biomass needs to be carried out. The  
16 similar lipid contents obtained for CO<sub>2</sub> and flue gas sparged cultures, can be substantiated with  
17 the studies of Chiu et al.<sup>35</sup> and Kumar et al.<sup>36</sup> However, the FAME profiles of CO<sub>2</sub> and flue gas  
18 aerated cultures showed significant variations, as discussed in Section 3.3.3. It was observed that  
19 there were no statistically significant differences in CO<sub>2</sub> fixation rate, photosynthetic efficiency,  
20 contents of chlorophylls and total carotenoids between CO<sub>2</sub> and flue gas sparged cultures of *C.*  
21 *minutissima* (Table 3). Therefore, these results demonstrate that the microalga *C. minutissima*  
22 can serve as a potential candidate for the remediation of flue gas and production of lutein and  
23 lipid. The process flow diagram for microalgal biorefinery model for the production of biofuels

1 and lutein with simultaneous flue gas carbon sequestration is shown in Fig.4. It is also shown  
2 that the defatted and depigmented biomass can further be subjected for carbohydrate extraction  
3 and subsequent bioethanol production by fermentation process.

### 4 **3.3.2. Simultaneous recovery of lutein and biodiesel**

5 The next step in the development of an integrated biorefinery model is to achieve the  
6 maximum possible recovery of both lutein and biodiesel simultaneously from the biomass. The  
7 scheme for the concurrent recovery of lutein and biodiesel (FAME) is shown in Fig. 5. Once the  
8 products of biomass were extracted using different binary solvent systems, the amount of water  
9 needed for proper phase separation was tested. The quantity of water required for methanol,  
10 ethanol and 2-propanol containing systems was found to be 10%, 15% and 30% (v/v),  
11 respectively. Table 4 shows the simultaneous recovery of lutein and FAME obtained by different  
12 solvent systems used. It was observed that different binary solvent mixtures showed almost  
13 similar recoveries of FAME ranging between 91.5% and 93.2%. This indicates the efficiency of  
14 hexane in extracting the lipids from aqueous alcoholic mixtures. It has to be noted that the polar  
15 solvents can easily penetrate the cell walls and thereby facilitate the non-polar solvent hexane for  
16 effective extraction of neutral lipids.<sup>22</sup> The maximum lutein recovery in aqueous phase was  
17 obtained in ethanol/hexane mixture of 94.3%, followed by methanol/hexane (90.5%) and 2-  
18 propanol/hexane systems (87.8%). The comparatively low lutein recovery by 2-propanol/hexane  
19 system might be attributed to higher water content (30%, v/v) in its aqueous phase than other  
20 solvent systems. Among different binary solvent mixtures tested for maximum recovery of both  
21 products from *C. minutissima*, ethanol/hexane system was found to give higher lutein and FAME  
22 contents (Table 4). This may be due to the existence of optimal intermolecular attractions and

1 relative solubility differences between the solvent molecules and intracellular products during  
2 extraction.<sup>37</sup>

3 The present findings are in agreement with that of Bai et al.<sup>14</sup>, which reported that the use of  
4 methanol/hexane system resulted in simultaneous recovery of 98% lipid and 90% chlorophyll  
5 from *Chlorella pyrenoidosa*. Despite the fact that the supercritical CO<sub>2</sub> extraction offers various  
6 advantages over classic solvent extraction methods, the study using such an expensive method  
7 for fractionation of lipids and pigments<sup>38</sup> resulted in a recovery of only 70% of the pigments  
8 along with the total extracted lipids. The pigments that were recovered during supercritical fluid  
9 extraction include astaxanthin, zeaxanthin/lutein, canthaxanthin and β-carotene. The lower  
10 recovery of pigments may be due to the entrainment of pigments by the lipids and subsequent  
11 reduction in the solubility of carotenoids towards the supercritical solvent.<sup>38</sup> In another study,  
12 Prommauk et al.<sup>13</sup> achieved almost complete recovery of lutein and biodiesel by performing  
13 simultaneous saponification and trans-esterification using alkali catalyst under appropriate  
14 conditions. However, a slightly higher concentration of alkali catalyst resulted in partial  
15 saponification of FAME that reduced the product yields. In addition, the complex product  
16 separation process may require additional equipments for the evaporation and recovery of  
17 solvents used. Hence, the method developed in the present study can be considered as simple and  
18 effective for the single-step extraction and separation of products using appropriate solvent  
19 mixture. Moreover, this study resulted in satisfactory yields of both the products and all the  
20 solvents used in the process can be recycled as shown in Fig. 5.

21 Thus, the current study rationally demonstrated the integration of biorefinery strategy  
22 involving concurrent production of lutein and biodiesel with flue gas CO<sub>2</sub> mitigation. This  
23 approach may effectively improve the competitiveness of commercially important microalgal

1 products. The preliminary economic assessment by Prommauk et al.<sup>13</sup> suggested that the process  
2 for concomitant production of lutein and biodiesel may be economically feasible. Further,  
3 sensitivity and economic analyses indicated that a maximum of 95 USD worth of lutein could be  
4 produced per kilogram of biodiesel. However, the detailed techno-economic assessment  
5 including the costs for capital, biomass production and subsequent downstream processes should  
6 be performed for commercial realization of lutein and biodiesel production, which is the focus of  
7 our future study.

### 8 **3.3.3. FAME composition analysis**

9 The predominant fatty acids of CO<sub>2</sub> and flue gas sparged cultures of *C. minutissima*, were  
10 identified as follows: palmitic (C16:0), stearic (C18:0), oleic (C18:1), linoleic (C18:2) and  
11 linolenic (C18:3) (Fig. 6a and b). These fatty acids have been reported to be more appropriate for  
12 biodiesel<sup>25,39</sup>. Table 5 shows the relative percentage composition of FAME of CO<sub>2</sub> and flue gas  
13 sparged cultures of *C. minutissima*. The total saturated fatty acid content of flue gas aerated  
14 cultures (67.4%) was found to be slightly higher than that of pure CO<sub>2</sub> sparged cultures (61.1%).  
15 On the others hand, the total unsaturated fatty acids of flue gas grown cultures (32.6%) was  
16 moderately decreased, as compared to pure CO<sub>2</sub> grown biomass (38.9%). A similar trend was  
17 also observed by Chiu et al.<sup>35</sup>, which reported that the levels of saturated fatty acid was increased  
18 from 48.6% to 62.3%, when the microalgae *Chlorella* sp. MTF-7 was grown using flue gas. It  
19 has to be noted that a higher level of saturated fatty acids may increase the stability of biodiesel,  
20 as the unsaturated fatty acids lack oxidative stability.<sup>34</sup> The presence of small amounts of  
21 unsaturated fatty acids such as C20:1 (1.1%) and C20:3 (2.7%), was also observed in this study,  
22 when *C. minutissima* was grown using flue gas. This may be due to the stress imposed by flue  
23 gas components, as demonstrated by Kumar et al.<sup>36</sup> Thus, the fatty acids with this obtained

1 composition may satisfactorily meet the desirable requirements of fuel properties such as cetane  
2 number, cold flow properties and oxidative stability.

#### 3 **4. Conclusion**

4 The present study convincingly demonstrated the development of an integrated biorefinery  
5 for microalgae based flue gas carbon sequestration and simultaneous production of commercially  
6 important microalgal products, namely, lutein and biodiesel. The application of ANN-PSO  
7 strategy for optimizing the critical process parameters resulted in significant enhancement in the  
8 productivities of lutein and lipid. The microalga *Chlorella minutissima*, when grown under the  
9 optimized conditions, could efficiently capture CO<sub>2</sub> from flue gas at a considerably higher  
10 fixation rate. Subsequent to this, the microalgae mediated flue gas CO<sub>2</sub> bioremediation process  
11 was satisfactorily integrated with the concurrent production of lutein and biodiesel. This study is  
12 expected to positively contribute to the contemporary scientific literature and it is supposedly the  
13 first report on process optimization and integration for the flue gas CO<sub>2</sub> sequestration with  
14 concomitant production of algal biomass, lutein and biodiesel.

#### 15 **Acknowledgments**

16 RD gratefully acknowledges the Department of Science & Technology (DST)-INSPIRE,  
17 Government of India for his fellowship. RD thankfully acknowledges Dr. Vivek Rangarajan for  
18 proof-reading the manuscript and Mr. Gunaseelan Dhanarajan for teaching the modeling and  
19 optimization technique, ANN-PSO. The authors gratefully acknowledge West Bengal  
20 Government-Department of Science & Technology (Project Grant No.560  
21 (SANC.)/ST/P/S&T/SG-5/2011; Date: 21-11-11) for the financial support. RD is also thankful to  
22 Mr. Lakshmikanta Dolai for his valuable assistance on flue gas operation and storage. The



1 authors are also grateful to Institute of Bio-resource and Sustainable Development, Imphal,  
2 India, and Indian Agricultural Research Institute, for providing their microalgal strains.

### 3 **References**

- 4 1. G. Markou and E. Nerantzis, *Biotechnol. Adv.*, 2013, 31, 1532-1542.
- 5 2. M. K. Lam and K. T. Lee, *Biotechnol. Adv.*, 2012, 30, 673-690.
- 6 3. Y. F. Shen, *Rsc Adv*, 2014, 4, 49672-49722.
- 7 4. J. M. Fernandez-Sevilla, F. G. Acien Fernandez and E. Molina Grima, *Appl. Microbiol.*  
8 *Biotechnol.*, 2010, 86, 27-40.
- 9 5. R. Slade and A. Bauen, *Biomass Bioenerg.*, 2013, 53, 29-38.
- 10 6. N. H. Norsker, M. J. Barbosa, M. H. Vermue and R. H. Wijffels, *Biotechnol. Adv.*, 2011, 29,  
11 24-27.
- 12 7. A. Nakanishi, S. Aikawa, S. H. Ho, C. Y. Chen, J. S. Chang, T. Hasunuma and A. Kondo,  
13 *Bioresour. Technol.*, 2014, 152, 247-252.
- 14 8. L. Brennan and P. Owende, *Renewable and Sustainable Energy Reviews*, 2010, 14, 557-577.
- 15 9. Y. Xie, S. H. Ho, C. N. Chen, C. Y. Chen, I. S. Ng, K. J. Jing, J. S. Chang and Y. Lu,  
16 *Bioresour. Technol.*, 2013, 144, 435-444.
- 17 10. E. J. Olguin, *Biotechnol. Adv.*, 2012, 30, 1031-1046.
- 18 11. Y. Huang, J. Cheng, H. X. Lu, R. Huang, J. H. Zhou and K. F. Cen, *Rsc Adv*, 2015, 5, 50851-  
19 50858.
- 20 12. I. Urreta, Z. Ikarán, I. Janices, E. Ibanez, M. Castro-Puyana, S. Castanon and S. Suarez-  
21 Alvarez, *Algal Res*, 2014, 5, 16-22.
- 22 13. C. Prommuak, P. Pavasant, A. T. Quitain, M. Goto and A. Shotipruk, *Chem. Eng. Technol.*,  
23 2013, 36, 733-739.

- 1 14. M.-D. Bai, C.-H. Cheng, H.-M. Wan and Y.-H. Lin, *J. Taiwan Inst. Chem. Eng.*, 2011, 42,  
2 783-786.
- 3 15. R. Dineshkumar, G. Dhanarajan, S. K. Dash and R. Sen, *Algal Res.*, 2015, 7, 24-32.
- 4 16. G. Dhanarajan, M. Mandal and R. Sen, *Biochem Eng J*, 2014, 84, 59-65.
- 5 17. J. Huang, L. H. Mei and J. Xia, *Biotechnol. Bioeng.*, 2007, 96, 924-931.
- 6 18. C. Posten, *Eng. Life Sci.*, 2009, 9, 165-177.
- 7 19. A. E. Abdelaziz, D. Ghosh and P. C. Hallenbeck, *Bioresour. Technol.*, 2014, 156, 20-28.
- 8 20. N. E. Craft and J. H. Soares, *J Agr Food Chem*, 1992, 40, 431-434.
- 9 21. F. Yang, C. Cheng, L. Long, Q. Hu, Q. Jia, H. Wu and W. Xiang, *Energy & Fuels*, 2015, 29,  
10 2380-2386.
- 11 22. Y. Li, F. G. Naghdi, S. Garg, T. C. Adarme-Vega, K. J. Thurecht, W. A. Ghafor, S. Tannock  
12 and P. M. Schenk, *Microb Cell Fact*, 2014, 13.
- 13 23. S. H. Ho, M. C. Chan, C. C. Liu, C. Y. Chen, W. L. Lee, D. J. Lee and J. S. Chang, *Bioresour.*  
14 *Technol.*, 2014, 152, 275-282.
- 15 24. E. G. Bligh and W. J. Dyer, *Can. J. Biochem. Physiol.*, 1959, 37, 911-917.
- 16 25. J. Sheng, R. Vannela and B. E. Rittmann, *Bioresour. Technol.*, 2011, 102, 1697-1703.
- 17 26. Y. Chisti, *Biotechnol. Adv.*, 2007, 25, 294-306.
- 18 27. A. R. Wellburn, *J. plant physiol.*, 1994, 144, 307-313.
- 19 28. S. H. Ho, C. Y. Chen and J. S. Chang, *Bioresour. Technol.*, 2012, 113, 244-252.
- 20 29. K. Maji, D. K. Pratihar and A. K. Nath, *Opt Laser Eng*, 2014, 53, 31-42.
- 21 30. F. Bohne and H. Linden, *Biochim. Biophys. Acta.*, 2002, 1579, 26-34.
- 22 31. L. H. Fan, Y. T. Zhang, L. H. Cheng, L. Zhang, D. S. Tang and H. L. Chen, *Chem. Eng.*  
23 *Technol.*, 2007, 30, 1094-1099.

- 1 32. L. Cheng, L. Zhang, H. Chen and C. Gao, *Sep. Purif. Technol.*, 2006, 50, 324-329.
- 2 33. M. Anjos, B. D. Fernandes, A. A. Vicente, J. A. Teixeira and G. Dragone, *Bioresour.*  
3 *Technol.*, 2013, 139, 149-154.
- 4 34. C. Y. Kao, T. Y. Chen, Y. B. Chang, T. W. Chiu, H. Y. Lin, C. D. Chen, J. S. Chang and C. S.  
5 Lin, *Bioresour. Technol.*, 2014, 166, 485-493.
- 6 35. S. Y. Chiu, C. Y. Kao, T. T. Huang, C. J. Lin, S. C. Ong, C. D. Chen, J. S. Chang and C. S.  
7 Lin, *Bioresour. Technol.*, 2011, 102, 9135-9142.
- 8 36. K. Kumar, D. Banerjee and D. Das, *Bioresour. Technol.*, 2014, 152, 225-233.
- 9 37. K. Ramluckan, K. G. Moodley and F. Bux, *Fuel*, 2014, 116, 103-108.
- 10 38. B. P. Nobre, F. Villalobos, B. E. Barragan, A. C. Oliveira, A. P. Batista, P. A. Marques, R. L.  
11 Mendes, H. Sovova, A. F. Palavra and L. Gouveia, *Bioresour. Technol.*, 2013, 135, 128-136.
- 12 39. G. De Bhowmick, G. Subramanian, S. Mishra and R. Sen, *Algal Res.*, 2014, 6, 201-209.

13

14

15

16

17

18

19

20

1

2

3 **Table 1**

4 Comparison of biomass, lutein and lipid productivities of chlorophycean microalgal strains

Microalgal strains	Biomass productivity (g L <sup>-1</sup> d <sup>-1</sup> )	Lutein productivity (mg L <sup>-1</sup> d <sup>-1</sup> )	Lipid productivity (mg L <sup>-1</sup> d <sup>-1</sup> )	Specific growth rate (μ, d <sup>-1</sup> )
<i>Scenedesmus</i> sp.	0.381 ± 0.012	2.05 ± 0.05	71.8 ± 3.5	1.36 ± 0.01
<i>Chlorella minutissima</i>	0.407 ± 0.015	2.37 ± 0.08	84.3 ± 4.1	1.44 ± 0.03
<i>Chlorococcum</i> sp.	0.314 ± 0.011	1.18 ± 0.06	81.9 ± 3.2	1.19 ± 0.02
<i>Chlorella</i> sp.	0.350 ± 0.014	1.49 ± 0.05	56.5 ± 2.7	1.27 ± 0.01

5

6 Data shown are the average of two experiments ± S.D.

7

8

9

10

11

12

13

14

15

16

17

1

2 **Table 2**

3 Central composite design for critical process parameters as independent process variables with  
 4 lutein productivity ( $\text{mg L}^{-1}\text{d}^{-1}$ ), lipid productivity ( $\text{mg L}^{-1}\text{d}^{-1}$ ) and biomass productivity ( $\text{g L}^{-1}\text{d}^{-1}$ )  
 5 as the responses

6

Run order	Light intensity ( $\mu\text{mol m}^{-2}\text{s}^{-1}$ )	CO <sub>2</sub> (%)	Flow rate ( $\text{mL min}^{-1}$ )	Lutein productivity ( $\text{mg L}^{-1}\text{d}^{-1}$ )	Lipid Productivity ( $\text{mg L}^{-1}\text{d}^{-1}$ )	Biomass productivity ( $\text{g L}^{-1}\text{d}^{-1}$ )
1	175	5	900	3.58	98.6	0.541
2	250	7.5	600	2.34	91.3	0.410
3	300	5	900	4.05	139.4	0.680
4	250	2.5	1200	4.11	131.4	0.568
5	100	7.5	600	1.12	72.6	0.335
6	250	2.5	600	3.77	112.5	0.445
7	175	5	1404	2.74	75.2	0.351
8	175	5	900	3.58	98.4	0.535
9	50	5	900	1.05	21.1	0.218
10	175	5	900	3.57	98.3	0.527
11	100	2.5	600	1.31	78.4	0.381
12	175	5	900	3.59	97.1	0.542
13	175	5	900	3.57	99.2	0.541
14	175	5	395	2.27	39.8	0.290
15	175	9.2	900	1.73	78.4	0.374
16	175	0.8	900	2.18	69.7	0.291
17	100	7.5	1200	1.4	73.5	0.330
18	250	7.5	1200	3.21	109.4	0.522
19	100	2.5	1200	1.36	81.2	0.473
20	175	5	900	3.59	97.8	0.541

7

8 Data shown are the average of two experiments

9

10

1

2 **Table 3**

3 Biomass growth characteristics and biochemical composition of *C. minutissima* cultivated using  
 4 CO<sub>2</sub> and flue gas.

Parameters	Units	pure CO <sub>2</sub> sparged	Flue gas CO <sub>2</sub> sparged
Biomass productivity	g L <sup>-1</sup> d <sup>-1</sup>	0.67 ± 0.018	0.64 ± 0.013
Lutein productivity	mg L <sup>-1</sup> d <sup>-1</sup>	4.32 ± 0.11	4.15 ± 0.09
Total lipid Productivity	mg L <sup>-1</sup> d <sup>-1</sup>	142.2 ± 5.6	139.3 ± 4.8
Specific growth rate	d <sup>-1</sup>	1.69 ± 0.02	1.58 ± 0.03
Total chlorophyll content	mg g <sup>-1</sup>	62.51 ± 3.4	59.64 ± 2.8
Total carotenoid content	mg g <sup>-1</sup>	8.58 ± 0.24	8.31 ± 0.19
Saturated fatty acid content	%	61.1 ± 2.3	67.4 ± 2.5
Unsaturated fatty acid content	%	38.9 ± 1.4	32.6 ± 1.1
Elemental analysis			
Carbon		48.59	48.98
Hydrogen	%	7.60	7.63
Nitrogen		8.41	9.73
Sulfur		0.74	1.13
CO <sub>2</sub> fixation rate	g L <sup>-1</sup> d <sup>-1</sup>	1.19 ± 0.03	1.15 ± 0.02
Photosynthetic efficiency	%	6.49	6.21

5

6

7

8

9

10

11

12

1

2 **Table 4**

3 Simultaneous recovery of lutein and fatty acid methyl ester (FAME) from flue gas sparged  
 4 cultures of *C. minutissima* by different solvent systems.

Method	Lutein content (mg per gram biomass)	% Lutein recovery	FAME yield (mg per gram CO <sub>2</sub> consumed)	FAME content (mg per gram biomass)	% FAME recovery
Control*	6.37 ± 0.11	-	56.97 ± 0.85	101.4 ± 1.5	-
Methanol: Hexane	5.76 ± 0.07	90.5	53.09 ± 0.66	94.5 ± 1.1	93.2
Ethanol: Hexane	6.01 ± 0.09	94.3	52.64 ± 0.47	93.7 ± 0.8	92.4
2-propanol: Hexane	5.59 ± 0.06	87.8	52.13 ± 0.41	92.8 ± 0.7	91.5

5 Data shown are the average of three experiments ± S.D.

6 \*Control: Lutein and FAME contents were extracted and analyzed separately using a known amount of biomass.

$$\% \text{ Product recovery} = \frac{\text{Product content obtained from simultaneous recovery}}{\text{Amount of product obtained from control method}}$$

7

8

9

10

11

12

13

14

15

16

17

18

1  
2  
3  
4  
5  
6

**Table 5**

Comparison of relative percentage composition of fatty acid methyl ester (FAME) of *C. minutissima* grown using CO<sub>2</sub> and flue gas

FAME	CO <sub>2</sub> sparged culture	Flue gas aerated culture
Capric (C10:0)	2.4	2.7
Lauric (C12:0)	6.8	6.6
Tridecanoic (C13:0)	2.2	0.8
Myristic (C14:0)	1.1	1.9
cis-10-Pentadecanoic (C15:1)	2.1	3.9
Palmitic (C16:0)	30.6	39.2
Palmitoleic (C16:1)	2.1	0.7
Heptadecanoic (C17:0)	0.7	0.6
cis-10-Heptadecanoic (C17:1)	1.9	1.8
Stearic (C18:0)	16.5	14.8
Oleic (C18:1n9c)	9.6	10.2
Linoleic (C18:2n6c)	8.7	6.5
$\alpha$ -linolenic ((C18:3n3)	14.5	5.7
Arachidic (C20:0)	0.8	0.8
cis-11-Eicosenoic (C20:1n9)	–	1.1
cis-11,14,17-Eicosatrienoic (C20:3n3)	–	2.7
Saturated FA (%)	61.1	67.4
Unsaturated FA (%)	38.9	32.6

7  
8



1  
2  
3  
4  
5  
6  
7  
8  
9  
10  
11  
12  
13  
14  
15  
16  
17  
18  
19  
20  
21  
22

## Figure Captions

**Fig.1.** (a) Regression plot of experimental and ANN predicted values. (b) Schematic diagram of optimized ANN topology consists of an input layer, a hidden layer with log-sigmoidal transfer function, and an output layer with pure linear transfer function. (c) Evolution of best fitness by PSO.

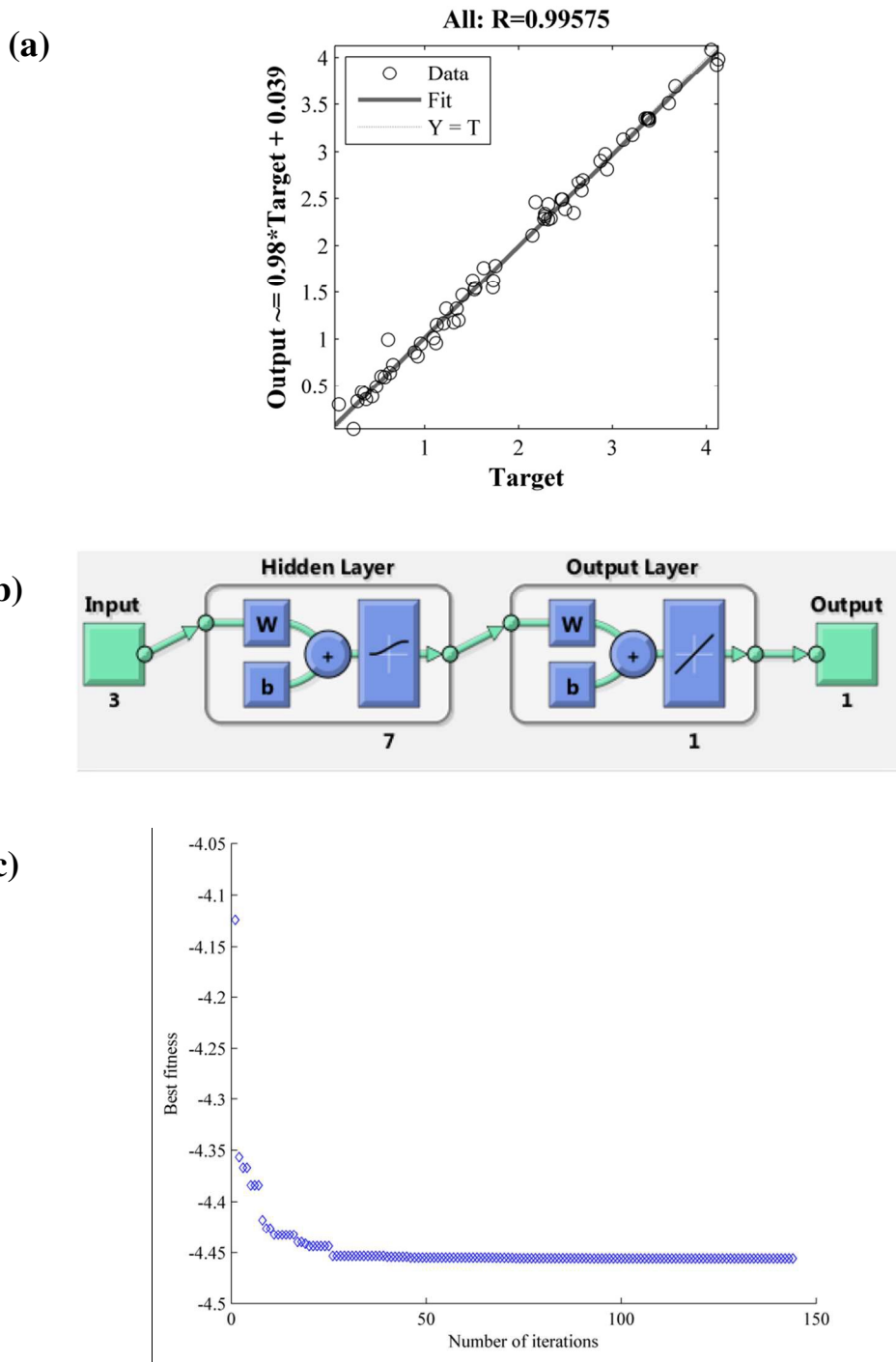
**Fig.2.** The characteristic profiles of photosynthetic efficiency, CO<sub>2</sub> fixation rate, and the productivities of lutein and lipid as a function of (a) light intensity, where CO<sub>2</sub> and flow rate were kept at their zero levels (b) CO<sub>2</sub> concentration, where light intensity and flow rate were held at their zero levels and (c) air flow rate, where light intensity and CO<sub>2</sub> were kept at their zero levels. (Zero levels: light intensity, 175  $\mu\text{mol m}^{-2} \text{s}^{-1}$ ; CO<sub>2</sub>, 5% and air flow rate: 900 mL  $\text{min}^{-1}$ ).

**Fig.3.** Time-course profiles of biomass production, CO<sub>2</sub> fixation rate, productivities of lutein and lipid, and nitrate uptake of *C. minutissima* cultivated using (a) pure CO<sub>2</sub> and (b) flue gas CO<sub>2</sub> under the optimized conditions.

**Fig.4.** Microalgal biorefinery model for the production of lutein and biofuels with concomitant flue gas CO<sub>2</sub> sequestration.

**Fig.5.** Schematic diagram for the concurrent recovery of lutein and biodiesel from *C. minutissima* that was grown using flue gas CO<sub>2</sub> under standardized process conditions

**Fig.6.** FAME profiles of *C. minutissima* cultivated using (a) pure CO<sub>2</sub> and (b) flue gas CO<sub>2</sub>

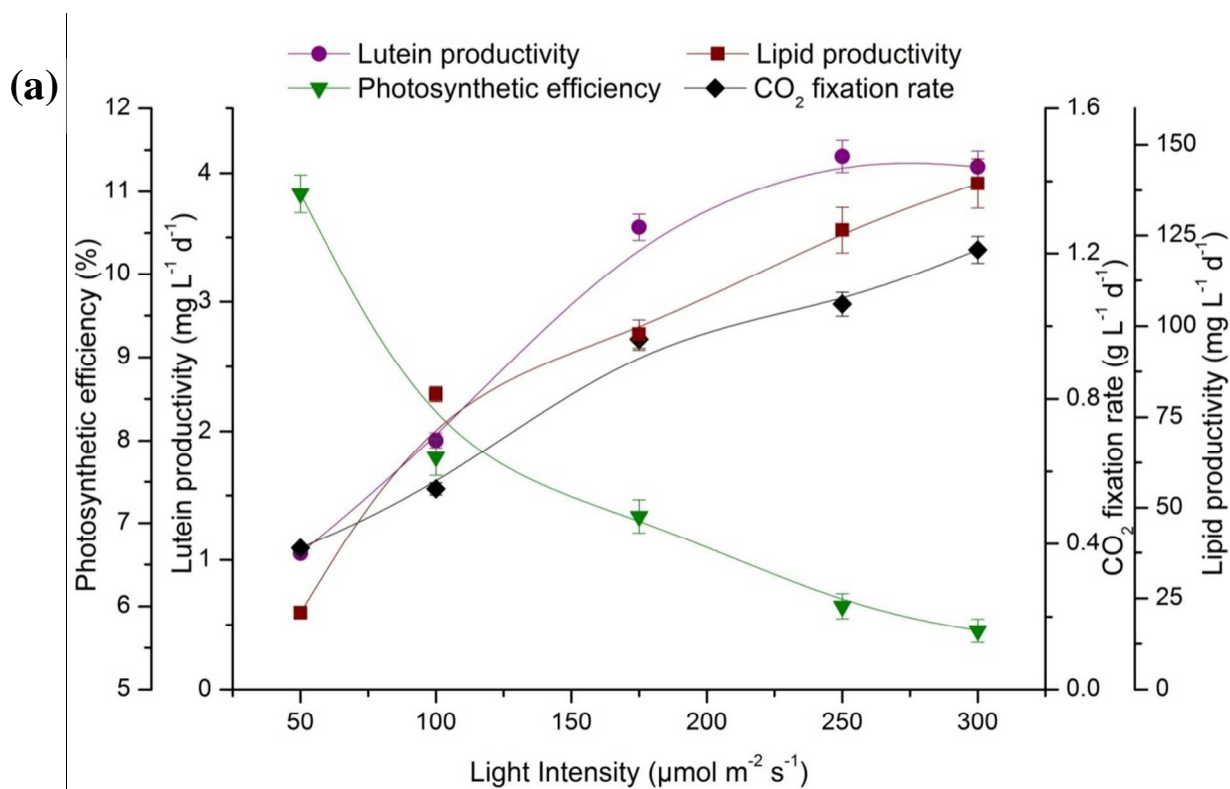
1 **Figure 1**

2

3

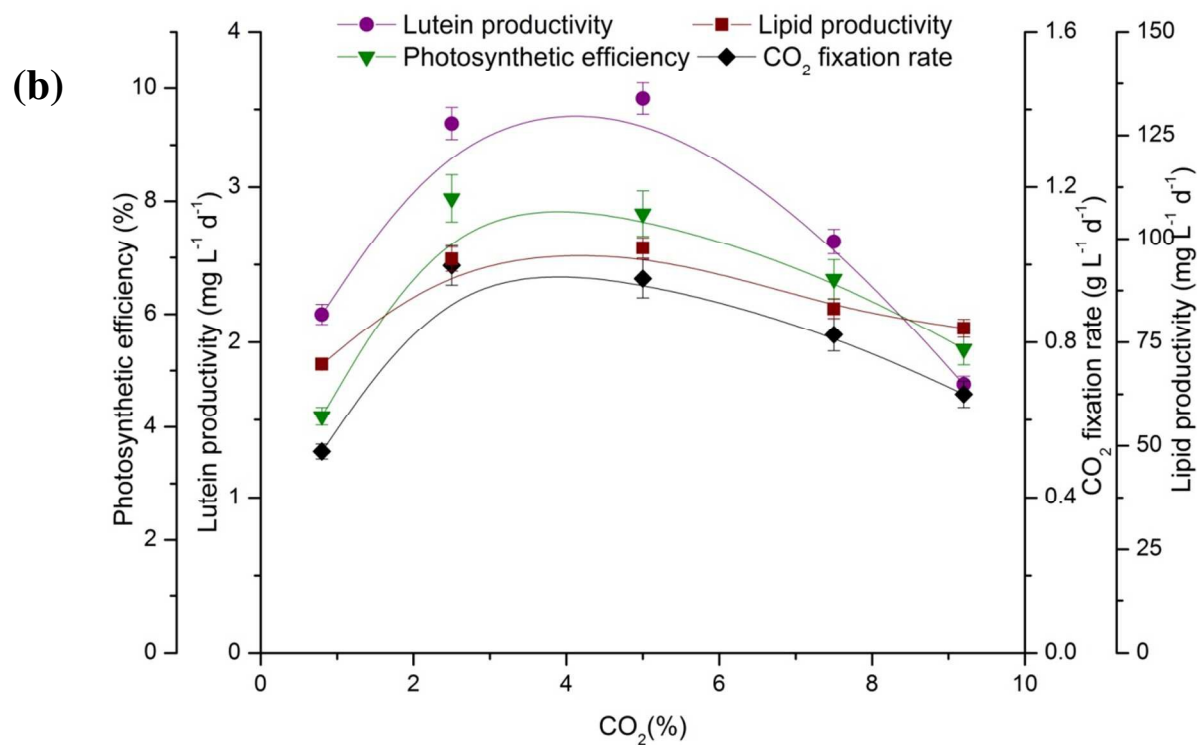
4

5 **Fig.1.** (a) Regression plot of experimental and ANN predicted values. (b) Schematic diagram of  
 6 optimized ANN topology consists of an input layer, a hidden layer with log-sigmoidal transfer  
 7 function, and an output layer with pure linear transfer function. (c) Evolution of best fitness by  
 8 PSO.

1 **Figure 2**

2

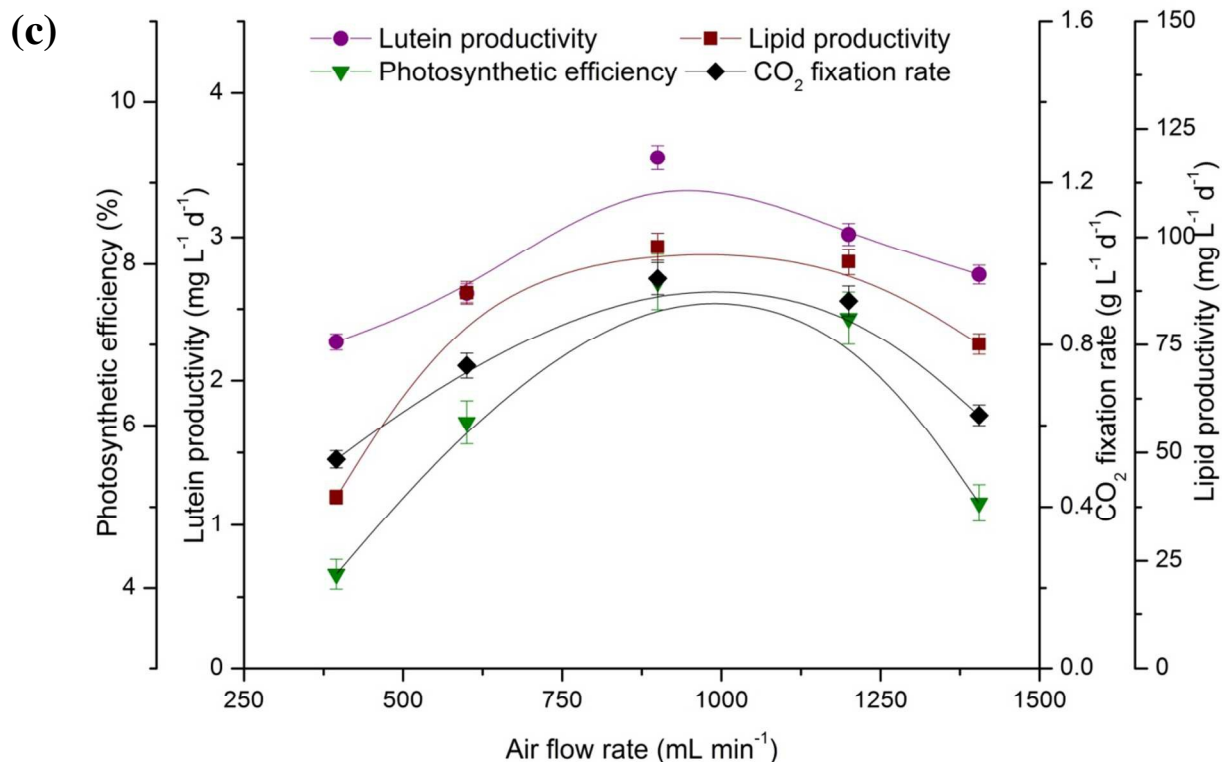
3



4

1

2



3

4

5 **Fig.2.** The characteristic profiles of photosynthetic efficiency, CO<sub>2</sub> fixation rate, and the

6 productivities of lutein and lipid as a function of (a) light intensity, where CO<sub>2</sub> and flow rate

7 were kept at their zero levels (b) CO<sub>2</sub> concentration, where light intensity and flow rate were

8 held at their zero levels and (c) air flow rate, where light intensity and CO<sub>2</sub> were kept at their

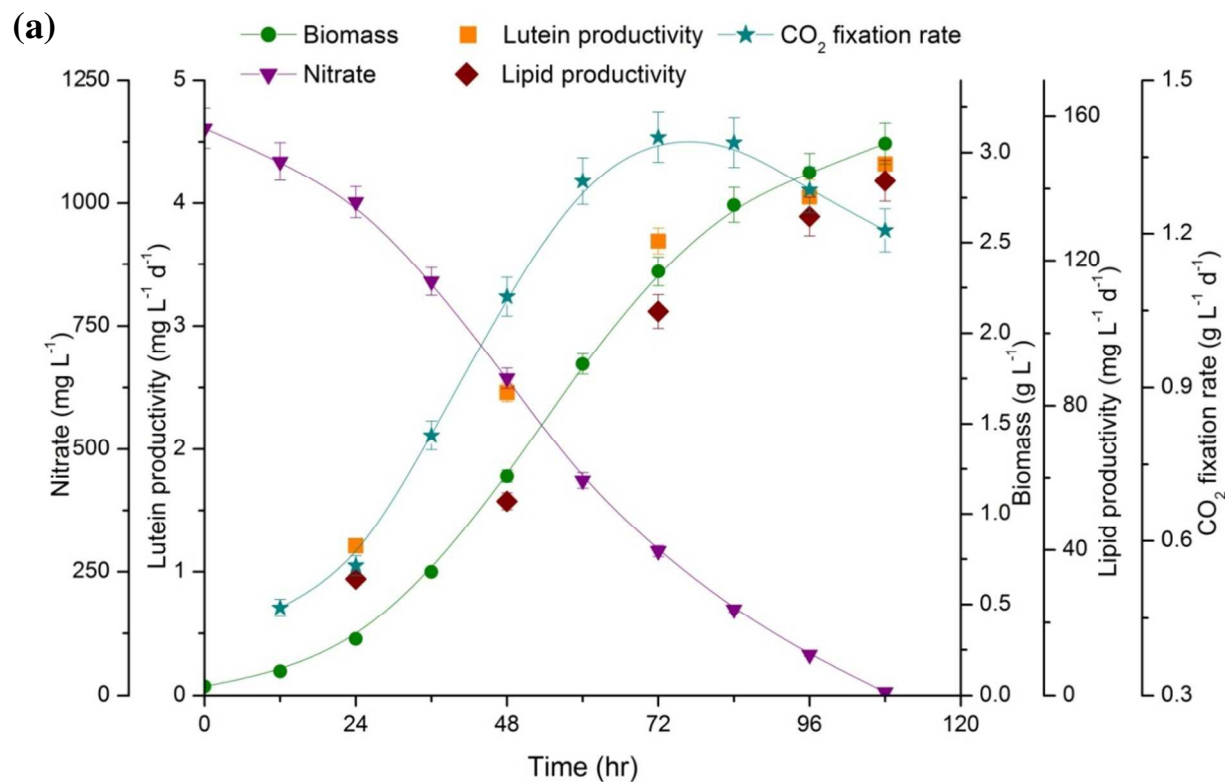
9 zero levels. (Zero levels: light intensity, 175 μmol m<sup>-2</sup> s<sup>-1</sup>; CO<sub>2</sub>, 5% and air flow rate: 900 mL

10 min<sup>-1</sup>).

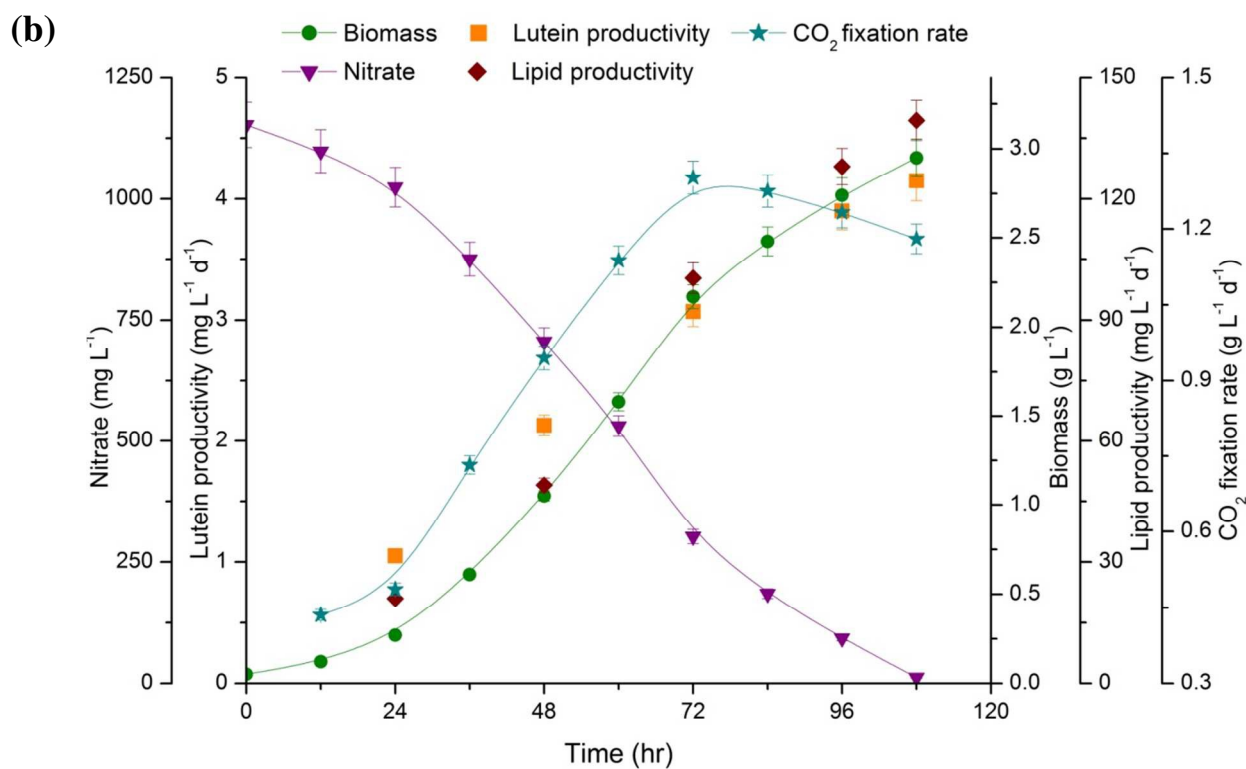
11

12

Figure 3



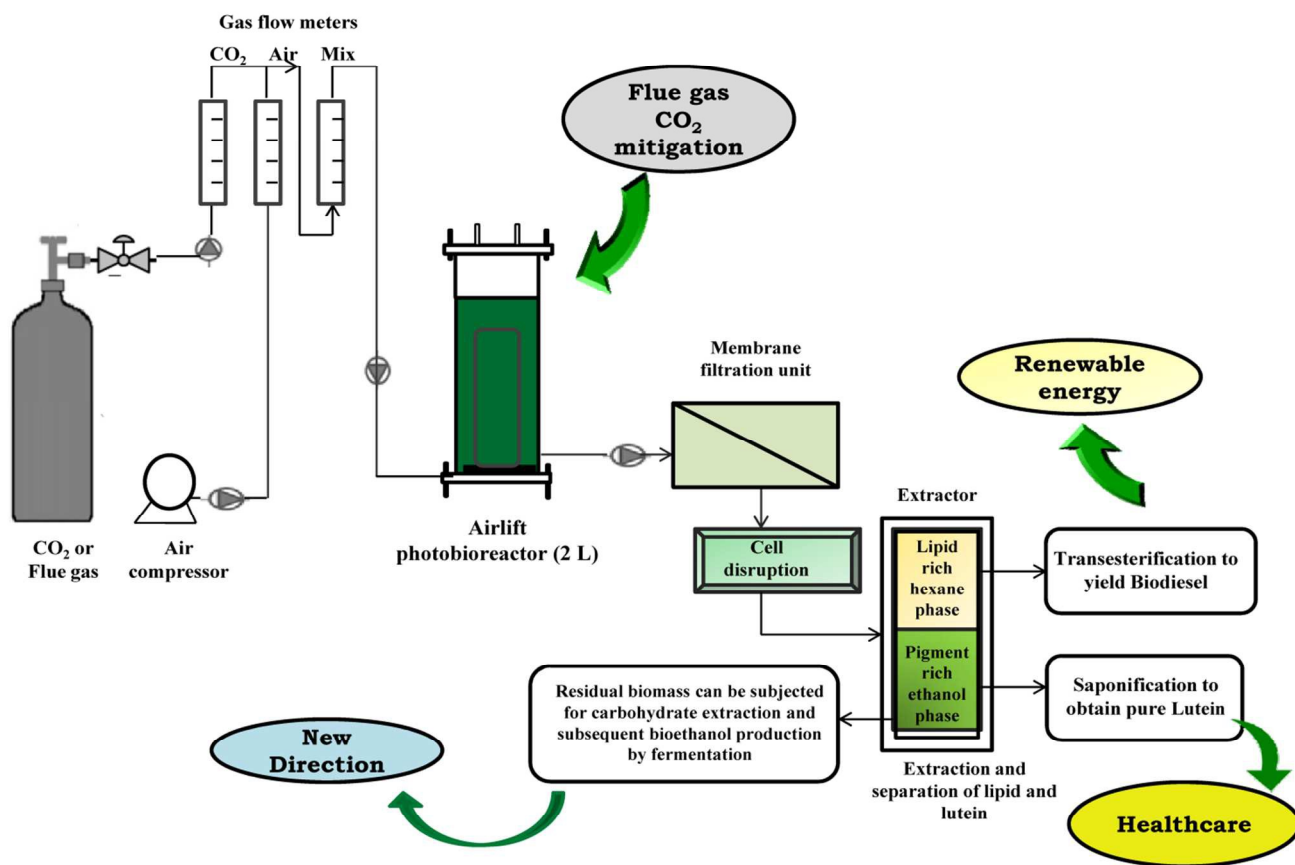
1



2

3 **Fig.3.** Time-course profiles of biomass production, CO<sub>2</sub> fixation rate, productivities of lutein and  
 4 lipid, and nitrate uptake of *C. minutissima* cultivated using (a) pure CO<sub>2</sub> and (b) flue gas CO<sub>2</sub>  
 5 under the optimized conditions.

Figure 4



2

3

4 **Fig.4.** Microalgal biorefinery model for the production of lutein and biofuels with concomitant  
 5 flue gas CO<sub>2</sub> sequestration

6

7

8

9

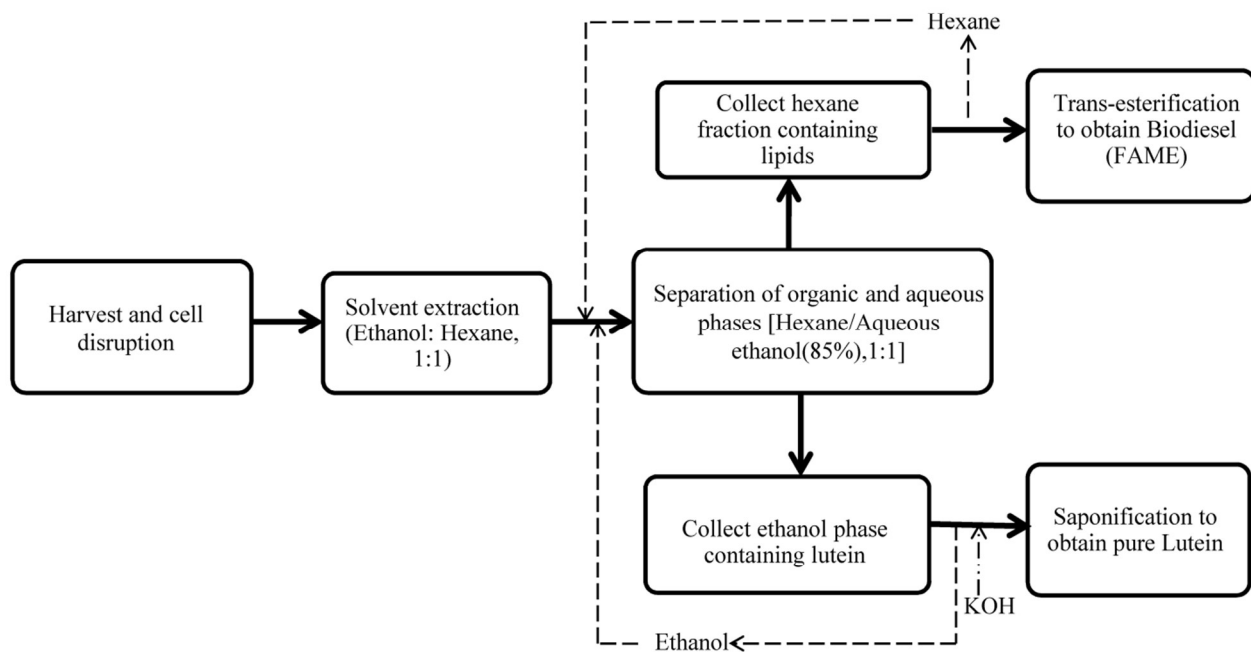
10

11

12

Figure 5

1



2

3 **Fig.5.** Schematic diagram for the concurrent recovery of lutein and biodiesel from *C.*  
4 *minutissima* that was grown using flue gas CO<sub>2</sub> under standardized process conditions

5

6

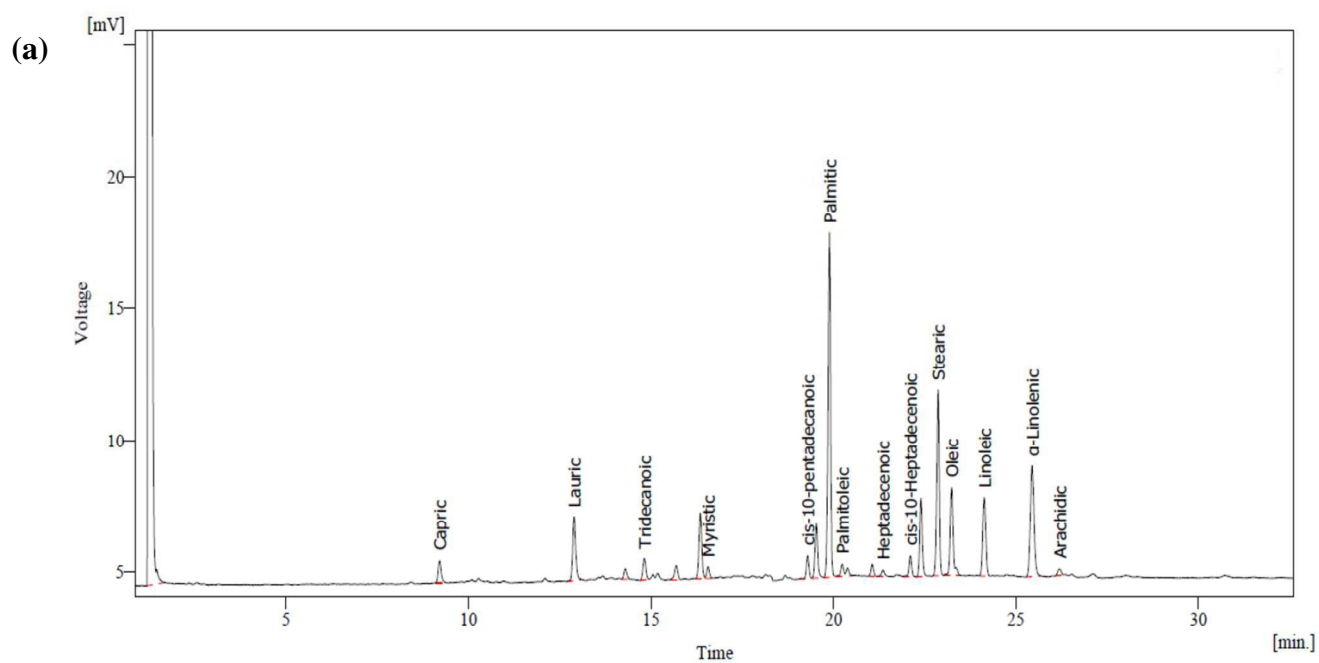
7

8

9

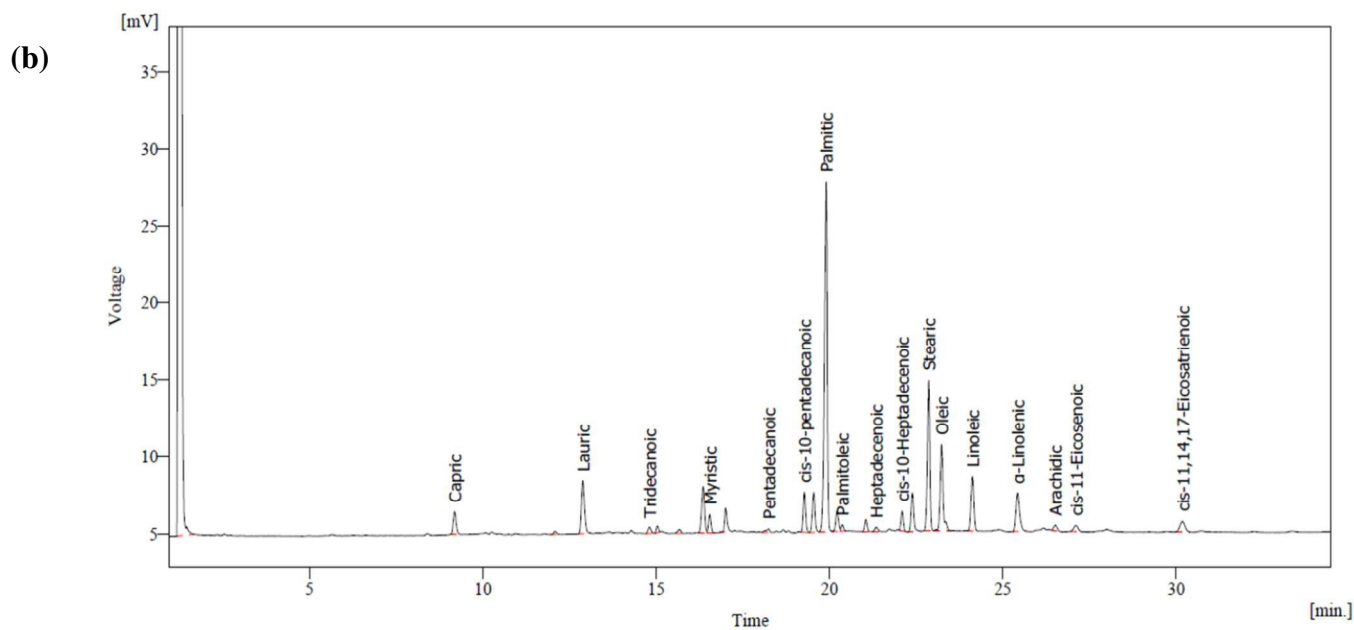
10

11

1 **Figure 6**

2

3



4

5

6 **Fig.6.** FAME profiles of *C. minutissima* cultivated using (a) pure CO<sub>2</sub> and (b) flue gas CO<sub>2</sub>